Effect of hydrogenating environment on crack growth and fractography peculiarities of the RPV steel

M.I. Hredil, O.Z. Student

5, Naukova Str., Karpenko Physico-Mechanical Institute of the NAS of Ukraine, Ukraine

mysya@ipm.lviv.ua

Keywords: reactor pressure vessel steel, heat affecting zone under cladding, fracture toughness, sub-critical crack growth, hydrogen embrittlement, intergranular fracture.

Abstract. The conditions for hydrogen-induced intergranular fracture in an artificially embrittled, low-alloyed reactor pressure vessel were investigated using fracture toughness and stress corrosion cracking tests. The specimens were taken from two locations: the heat affected zone (HAZ) beneath the cladding and the base material directly below the HAZ. A hydrogenating system allowed the tests to be carried out on both pre-hydrogenated specimens or with continuous hydrogenation during testing itself. The fracture and stress corrosion cracking tests demonstrated a detrimental effect of both hydrogenation during testing and pre-hydrogenation on the J_{Ii} or K_{Ith} levels for the HAZ and sub-HAZ base materials. This implies that susceptibility to sub-critical cracking may need to be considered for real or postulated defects in embrittled components subject to such conditions over extended periods. The SSC results suggest that the base material is more sensitive to hydrogen embrittlement effects than the HAZ; this is considered to be linked to the presence of segregation bands in the former. Fractographic examination shows that the effect of hydrogen becomes apparent as classical embrittlement (cleavage, intercrystalline or intergranular fracture) only in the transition regime (ambient temperature for this steel). At 120°C (upper shelf) hydrogen charging appears to reduce the energy needed for ductile tearing along slip planes, with much finer dimpling than found in the absence of environment effects. There is some evidence that pre-absorbed hydrogen favours local cleavage. Differences in fracture mode for hydrogenated specimens at the two temperature levels is also thought to be connected with a competition between two types of hydrogen transport to the crack tip – by grain boundary diffusion and via mobile dislocations in the bulk. The former is prevalent at ambient temperature when intergranular fracture is observed.

Introduction

The conditions for hydrogen-induced intergranular fracture in an artificially embrittled, low-alloyed reactor pressure vessel were investigated using fracture toughness and stress corrosion cracking tests. The specimens were taken from two locations: the heat affected zone (HAZ) beneath the cladding and the base material directly below the HAZ. A hydrogenating system allowed the tests to be carried out on both pre-hydrogenated specimens or with continuous hydrogenation during testing itself.

Material and test methods

The material used in the study was taken from the so-called NESC-I cylinder [1], which was fabricated from ASTM A508 Class 3 steel (0.23C, 0.23Si, 1.32Mn, 0.011S, 0.012P, 0.08Cr, 0.50Mo, 0.73Ni) subjected to a non-standard heat treatment to simulate embrittlement of a reactor pressure vessel steel at the end-of-life.

For the testing programme 0.5CT specimens with a reduced thickness of 10 mm were machined from two locations in the cylinder wall: heat affected zone (HAZ) and base material i.e. just beneath HAZ. The reason for considering this particular base material location is that it corresponds to that where

extensive intergranular cracking was observed at the large sub-clad defect in the NESC-I test. The orientation of all the specimens was L-T. Attention was mainly focussed at the 120°C temperature level, which corresponds to the time in the NESC-I thermal shock transient at which the crack driving force at the large sub-clad defect was approaching its peak. At this point the test instrumentation also indicated that an event may have taken place, although it cannot be excluded that the intergranular extension took place prior to testing. To study the effect of hydrogen on the fracture properties in this upper transition regime, the specialised test system was used. This consists of a tensile test machine equipped with an autoclave to allow continuous hydrogenation of the specimen in a heated solution using an electrochemical process [2]. The following test environments were used:

- Saturated $CaCl_2$ solution at 120°C, with cathodic charging at current densities of 10^{-5}, 10^{-3} and 10^{-1} A/cm^2.
- 0.3% NaCl (pH6.5) + 2 g/l thiourea at the current density of 10^{-1} A/cm^2.
- H_2SO_4 solution (pH 0) + 2 g/l thiourea at the current density of 10^{-1} A/cm^2. This environment was used for both pre-hydrogenation and hydrogenation during testing. In the case of the former, the specimens were plated using a two layer process (first a Ni layer as a substrate, then a Cu layer as a barrier to hydrogen desorption), before testing. This allows the effect of absorbed hydrogen on the mechanical behaviour of specimens to be studied.
- Silicon oil at 120°C as an inert atmosphere (this modelled the tests in air at increased temperature and was used to provide a control against which the effect of hydrogenation could be judged).

Three types of tests were used: fracture toughness, stress corrosion cracking rising displacement (SSC-RD) and stress corrosion cracking constant load tests (SCC-CL):

a) Fracture toughness tests: during the tests the load (P) vs. load-line displacement (V_{LL}) data were recorded and subsequently used for estimating the J-integral [2] and associated J–R curve, following a multi-test procedure similar to that specified in ASTM E1820. The depths of the pre-fatigue and final crack fronts were measured from the broken specimens.

b) SSC-RD tests: these were performed in a similar way to the fracture toughness experiments but with a much slower loading rate (the load-line displacement rate V_{LL} was 10 μm/h compared to 1 mm/min for the fracture tests).

c) SCC-CL tests: these were performed by ramping the load to a pre-defined level and holding this constant. At the end of the test (due to fracture or after a fixed period of time) the amount of sub-critical crack growth was measured.

The test matrix included: a) fracture toughness and SCC-RD tests at 120°C and SCC-CL tests at ambient temperature in hydrogenating solutions and different current densities of cathodic charging; b) fracture toughness tests inert in silicon oil at 120°C, with and without preliminary hydrogenation, and c) fracture toughness, SCC-RD and SCC-CL constant loading tests in air at ambient temperature after preliminary hydrogenation. Test type (a) addressed possible cracking due absorption of external hydrogen, while types (b) and (c) assessed the role of internal hydrogen.

The fracture surfaces of the majority of the test specimens were examined using optical and scanning electron microscopy to determine the fracture mode.

Test results

Fracture toughness. Table 1 summarises the J_{Ii} and $J_{I0.2}$ values determined from the intersection of a linear fit to the J–Δa data with the blunting line and the 0.2 mm offset line respectively. The blunting line slope is $2\sigma_y$, with σ_y (flow stress) = 720 and 536 MPa for the HAZ and base materials respectively.

For the HAZ specimens results obtained with the minimum hydrogen charging intensity ($j = 10^{-5}$ A/cm^2) are comparable to those from the tests in the "inert" silicon oil environment. However more intensive hydrogenation ($j = 10^{-3}$ A/cm^2) is found to decrease the crack growth resistance. A similar effect was found in the tests on the base material specimens. The lower slope of the J–R

curve for $j = 10^{-1}$ A/cm^2 is indicative of the low tearing resistance at a very high level of hydrogen charging. Overall the HAZ specimens produced somewhat lower toughness values at this temperature than those of the base material.

Table 1. Fracture toughness values at 120°C for HAZ and base materials

Test conditions		HAZ		Base	
		J_{Ii}	$J_{I0.2}$	J_{Ii}	$J_{I0,2}$
		N/mm		N/mm	
$CaCl_2$ solution	$j = 10^{-5}$ A/cm^2	162	218	197	256
	$j = 10^{-3}$ A/cm^2	126	184	147	206
	$j = 10^{-1}$ A/cm^2	–	–	68	75
Silicon oil		162	218	–	–

SCC-RD tests. In all cases the cracking initiated while the $P - V_{LL}$ curves were still linear, allowing use of a LEFM approach to calculate a threshold SIF $K_{Ith.}$ The values obtained are presented in Table 2. For the 120°C temperature level, the K_{Ji} values were obtained by converting the values of J at crack initiation (J_{Ii}) using the standard relationship: $K_j = \sqrt{[E \times J(1-\nu^2)]}$, valid for plane strain conditions. In the case of the HAZ material the value of J_{Ii} = 162 N/mm from the test at 120°C in silicon oil is used, giving K_{Ji} = 194 MPa$\sqrt{\text{m}}$; for the base material we use J_{Ii} = 197 N/mm from the fracture test with the lowest current density (for which there appeared to be little or no effect of hydrogenation), giving K_{Ji} = 214 MPa$\sqrt{\text{m}}$. At the 20°C level, no fast fracture tests were performed in this study and therefore results from the NESC-I programme are used [1].

Table 2. Results of SCC-RD tests, including fast fracture reference values

Temperature, °C	Pre-hydrogenating treatment	Test conditions	K_{Ith}, MPa$\cdot\sqrt{\text{m}}$	
			HAZ	Base
120	none	solution $CaCl_2$, $j = 10^{-5}$ A/cm^2	64	55
	none	solution $CaCl_2$, $j = 10^{-1}$ A/cm^2	43	46
	2 h at 10^{-1} A/cm^2	silicon oil (inert)	57	47
	50 h at 10^{-1} A/cm^2	silicon oil (inert)	–	44
	none	reference fast fracture[1]	194[1]	214[1]
20	2 h at 10^{-1} A/cm^2	air	–	39
	150 h at 10^{-1} A/cm^2	air	31	–
	none	reference fast fracture[2]	65[2]	40[2]

[1)] The reference value at 120°C is derived from fracture tests J_{Ii} results for inert or quasi-inert conditions.
[2)] The reference value at 20°C is derived from Master Curve 5% failure probability curves, after size correction from 25 to 10 mm specimen thickness.

Comparing the data in Table 2 the following observations can be made:

- At 120°C both base and HAZ specimens produced K_{Ith} values well below the reference level, indicating their sensitivity to hydrogen cracking even at the minimum current density (10^{-5} A/cm^2). This effect was similar for both continuous and pre-hydrogenated specimens.

- At 20°C the material also shows evidence of degradation of the threshold for cracking due to hydrogen, in that all the tests provided indications of cracking at K levels below the Master Curve lower bound value used here as a reference. The decrease is modest in the case the base material (2 h pre-hydrogenation). However the HAZ specimen was subject to a much longer pre-hydrogenation treatment (150 h) and has produced a K_{Ith} estimate substantially below the reference toughness value.

SCC-CL tests. These tests were intended to check the morphology of any sub-critical crack growth; no measurements of growth rate were made. Base material and HAZ specimens were tested at ambient temperature with hydrogen charging at the current density of 10^{-1} A/cm^2 and a sustained constant load sufficient to produce a crack stress intensity value (50 MPa$\sqrt{\text{m}}$) i.e. slightly above the K_{Ith} level seen in the SCC-RD tests. The HAZ specimen was tested in a H_2SO_4 solution + 2g/l thiourea with a current charging density of 10^{-1} A/cm^2 and completely fractured after 310 min. The base material specimen was tested in a less aggressive 0.3% NaCl solution + 2 g/l thiourea. In this case crack growth of about 1.5 mm maximum was obtained after 430 h, without fracture of the specimen. Additionally one base material specimen was tested at ambient temperature after 150 h of preliminary hydrogenation in a H_2SO_4 solution + 2g/l thiourea with a current charging density of 10^{-1} A/cm^2.

SSC-RD fractography. For the tests at 120°C with continuous hydrogen charging the extent of cracking was delimited by secondary cracks (Fig. 2*a*), and was found to decrease with increasing current density values, presumably due to the corresponding increase in intensity of hydrogenation making conditions more favourable for crack branching. **Ошибка! Источник ссылки не найден.**2*b* shows an example for the base material specimen. One peculiarity was the presence of occasional large dimples, with diameters from 50 to 200 μm, as shown in Fig. 2*c*, again for the base material specimen. The dimple walls are themselves covered by networks of smaller dimples, at the bottom of which one finds features with sizes comparable to the grain size (20 to 30 μm). It is interesting that size and spacing of these big dimples corresponds to that of the segregation bands observed in this steel during the original NESC investigations [3].

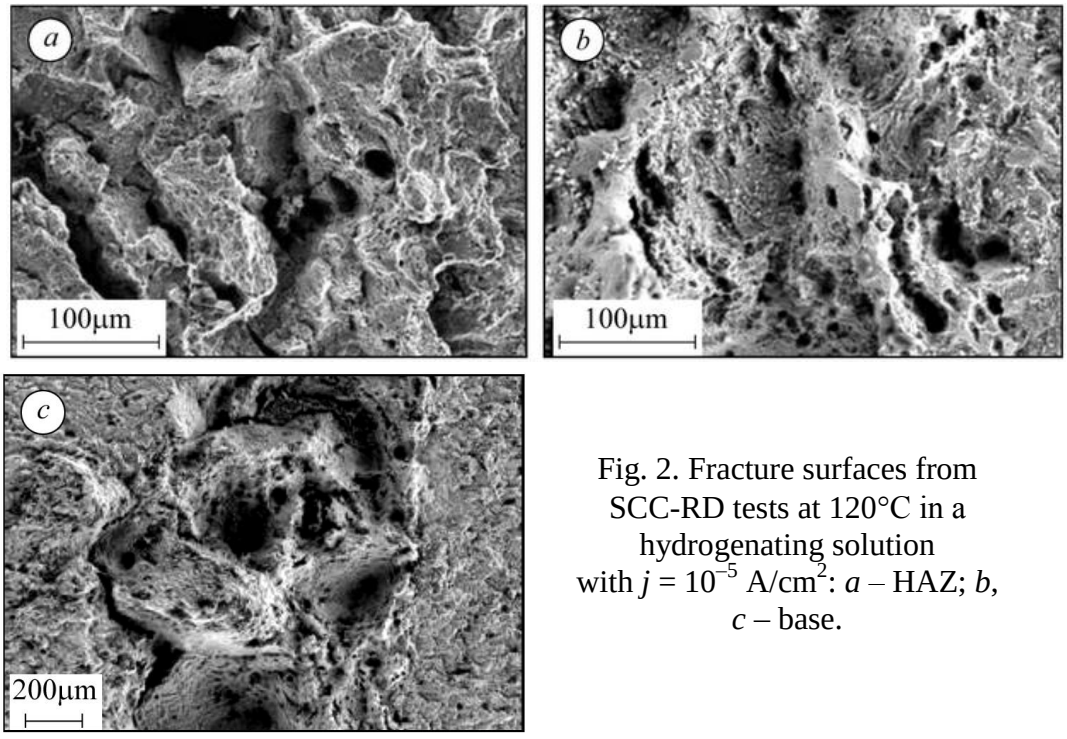

Fig. 2. Fracture surfaces from SCC-RD tests at 120°C in a hydrogenating solution with $j = 10^{-5}$ A/cm^2: *a* – HAZ; *b*, *c* – base.

Concerning the specimens tested in inert conditions at 120°C after pre-hydrogenation (2 h), the fracture mode was ductile in character, but the zone of smooth tearing in the initial stage of sub-critical crack growth was no longer present for the base material. Deep secondary cracks were observed along the crack front, with their edges entirely covered by equiaxed microdimples with a diameter of about 5 to 10 μm. As growth continues the dimples become larger (10 to 20 μm) and slightly elongated, covering large (~500 μm) flat facets. These shallow dimples have traces of shear deformation at the bottom as a result of intensive plastic local deformation (Fig. 3*a*). Overall, the hydrogen absorbed during the pre-treatment did not appear to cause any brittle-type features on the fracture surface of the base material. The fracture surfaces of specimens with longer pre-hydrogenation (50 h) showed irregular tearing to depths of 50 to 70 μm from the pre-crack front. These areas are covered by traces of shear deformation and terminate with discontinuous secondary cracking. Some isolated pockets of cleavage with characteristic "river" patterns were also observed (Fig. 3*b*), which is a typical feature of embrittlement due to pre-absorbed hydrogen.

Strong differences in fracture morphology were observed between base material and HAZ in SCC-RD tests at ambient temperature after preliminary hydrogenation (2 h and 150 h respectively). The fracture surface from the HAZ specimen is characterised by cleavage features on grain facets with interspersed shear lips, and a total absence of the intergranular fracture (Fig. 4*a*). This is attributed to the preliminary hydrogenation.

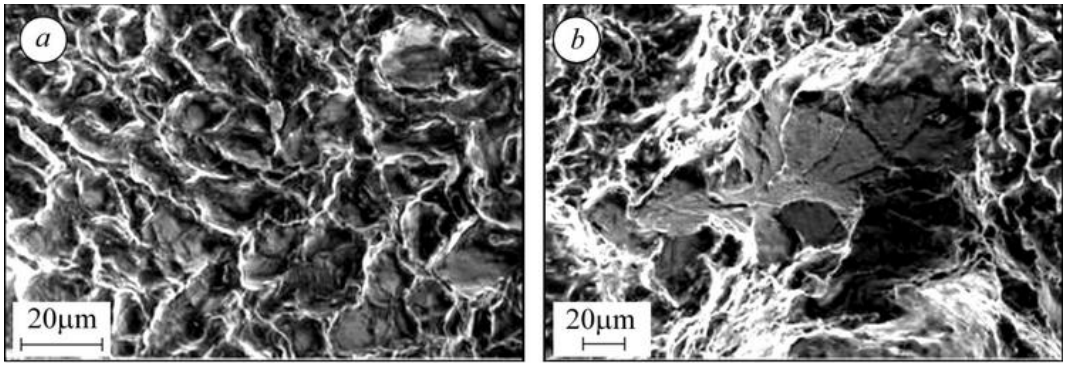

Fig. 3. SEM of base material specimens after SCC-RD tests at 120°C in silicon oil after pre-hydrogenation at $j = 10^{-1}$ A/cm$^{2.}$ for 2 h (*a*) and 50 h (*b*).

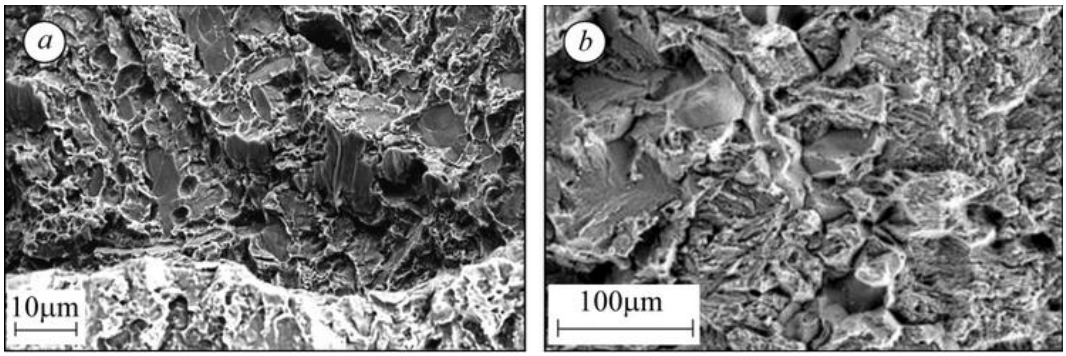

Fig. 4. Fracture surfaces from SCC-RD tests at ambient temperature after pre-hydrogenation: *a* – HAZ, 150 h; *b* – base, 2 h.

On the other hand the fracture surface of the base material after much less pre- hydrogenation (2 h) is a mix of inter- and transgranular features (Fig. 4*b*). A zone of intergranular facets was observed just after the fatigue pre-crack and at a depth of 2 to 4 mm from the side of specimen (this contrasts

with the pure cleavage observed in a fast fracture test specimen as shown in **Ошибка! Источник ссылки не найден.**1*d*). The morphology of the rest of the facets (not-intergranular) reflects details of the bainitic microstructure, but they make up only a small part of the overall cleavage fracture morphology, which fans out from points on the crack front.

SCC-CL tests fractography. The fracture surface of the HAZ specimen after the SCC-CL test at ambient temperature with continuous hydrogenation showed a mix of inter- and transgranular features (Fig. 5*a*). Although transgranular fracture dominated at the transition from the pre-fatigue crack tip to SCC-driven growth (Fig. 5*b*), the intergranular part increased moving inwards. This indicates that at the beginning of this type of test hydrogen diffusion is insufficient to cause embrittlement close to the crack tip i.e. within a distance comparable to the grain size. It further noted that fracture morphology identified above as transgranular is actually along bainitic crystallites and, as such, has an intercrystalline character. Therefore hydrogen diffusion also had an embrittling effect during crack initiation.

For base material hydrogenated under softer conditions, practically pure intergranular fracture was observed (Fig. 5*c*). Moreover the fracture surface of the pre-hydrogenated base material specimen showed a mix of inter- and transgranular features (Fig. 5*d*), with a higher proportion of the former. Similarly to the HAZ specimen test described above, the so-called transgranular features frequently take the form of fracture along bainitic crystallites, implying that there is a hydrogen embrittlement effect at both the grain and bainitic crystallite boundaries.

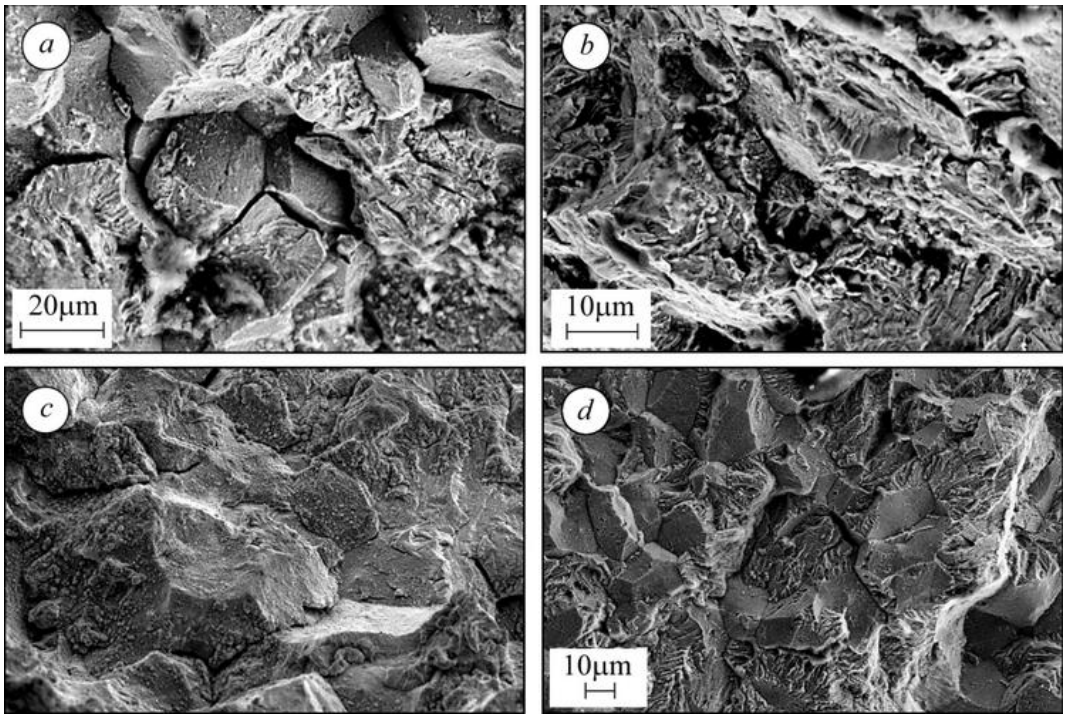

Fig. 5. Fracture surfaces from SCC-CL tests at ambient temperature during hydrogen charging (*a*–*c*) in H_2SO_4 solution + 2g/l thiourea (*a*, *b*) and 0.3% NaCl + 2g/l thiourea (*c*) and after pre-hydrogenation (*d*) at the current density of 10^{-1} A/cm^2.

Discussion

The main goal of this work was to investigate the susceptibility of artificially embrittled pressure vessel steel to hydrogen-induced fracture, in particular intergranular cracking. Initially the focus was on the fracture toughness and SCC-RD tests performed at a temperature in the upper shelf with continuous hydrogenation by cathodic charging. The results confirmed the detrimental effect of hydrogen charging and increasing the current density during testing caused J_{Ii} or K_{Ith} level to decrease. The effect of

hydrogenation was particularly pronounced in the SCC-RD tests, with the measured K_{Ith} values lying well below the fast fracture reference level, presumably because the slower loading rate facilitated hydrogen transport to the crack tip region. Increasing the duration of the pre-hydrogenation from 2 to 50 h did lead to some signs of local cleavage, drawing attention to the influence role of internal hydrogen on the fracture energy. These results imply that susceptibility to sub-critical cracking may need to be considered for real or postulated defects subject to such conditions over extended periods.

Concerning the relative sensitivity of the two material zones to hydrogenation effects, comparison of the *J–R* fracture behaviour at 120°C showed the HAZ material has a somewhat lower fracture resistance than the base material. In terms of threshold to sub-critical cracking (K_{Ith}), the results of the SCC-RD tests suggest that the base material may be slightly more sensitive to hydrogenation effects. Although the fracture mechanism is essentially the same for both materials, the HAZ specimen fracture surfaces did not show the large, deep dimples seen on those for the base material specimens. This appears related to the presence in the latter of segregation bands oriented perpendicularly to the fracture surface and these features may play a role in the slight observed reduction of K_{Ith}.

In contrast to the tests at 120°C, the SCC tests at ambient temperature i.e. in the ductile to brittle transition regime, produced a different fracture mechanism, which depended on both the microstructure (base or HAZ) and the test conditions. The HAZ specimen fracture surfaces did not show intergranular fracture in rising displacement SCC-RD tests after pre-hydrogenation (internal hydrogen) but had mixed intergranular and transgranular features in the constant loads tests with hydrogen charging (external hydrogen). The base material was found to be more sensitive to hydrogen embrittlement than HAZ one. For example, intergranular fracture was the characteristic feature of sub-critical crack growth in the base material SCC-RD specimen tested after 2 h of pre-hydrogenation. In contrast such features were not found on the HAZ specimen even after 150 h of preliminary hydrogenation (see Fig. 4).

These differences reflect differences in the locations of maximum hydrogen concentration, superimposed on the normal transition in fracture behaviour for low-alloy steels. For the fracture toughness and SCC-RD tests at 120°C the dislocation mechanism of hydrogen transport dominates, occurring preferentially along the principal sliding planes. This promotes tearing along these planes, with the energy required correlating inversely to the intensity of hydrogenation. Moving to the lower temperature affects the intensity and character of hydrogen diffusion. Transport to a crack tip by grain boundary diffusion becomes competitive with that via dislocations in the bulk. This is consistent with the evidence of limited intergranular cracking, in combination with an overall cleavage fracture mode expected in the transition range. In the SCC-CL tests it could be expected that this grain boundary effect (and resulting intergranular fracture) could become prevalent if the hydrogenation is sufficiently intensive or if the metal is very sensitive to such a fracture mode.

This hypothesis concerning the increasing role of grain boundary hydrogen diffusion with respect to that via dislocations in the bulk is consistent with the fracture morphologies seen in the SCC-RD and SCC-CL tests at ambient temperature. These mechanisms of hydrogen transport should depend on the relative hydrogen concentrations on the grain boundaries and in the bulk, with the latter determining whether the fracture mechanism is trans- or intergranular. In the case of the SCC-RD tests the amount of intergranular fracture decreases as one moves inwards from pre-fatigue crack front. This can be explained by an increase of hydrogen transport by the dislocation mechanism, since the slow raising displacement provides a continuous source of mobile dislocations which can redistribute hydrogen from grain boundaries to inside of grains. This mechanism should intensify with crack growth as the *K* level increases, causing a decrease in the grain boundary hydrogen concentration and, correspondingly, of the proportion of intergranular fracture. On other hand, for the SCC-CL tests, when the dislocation mechanism of hydrogen transport is less significant, the percentage of intergranular fracture increases in the direction of crack growth due to the predominance of grain boundary diffusion. Here one should take into consideration that the increase of sub-critical fracture zone size means that more grain boundaries

are subject to 3-D tensile stresses. This in turn promotes grain boundary hydrogen diffusion flow and increases the likelihood of intergranular fracture.

One further observation: the above analysis of the fracture mechanism was made in terms of transgranular and intergranular fracture modes. However, in the case of transgranular fracture it was possible to distinguish between cleavage on sliding planes and intercrystalline fracture along bainite boundaries. The latter is a type of crystalline boundary fracture like intergranular fracture, but on the scale less than a grain size. This may need to be treated as a separate phenomenon, whose occurrence depends on the microstructure and the level of hydrogenation i.e. if hydrogenation is more intense or the material is more sensitive to hydrogen cracking the intergranular fracture is observed; for less intense hydrogenation and lower material susceptibility, bainite boundary fracture may occur.

Turning lastly to the consequences of the above results on our understanding of the instances of intergranular cracking at the large sub-clad defect that occurred in the NESC tests, it has been assumed that this cracking took place during the test transient, when the inner surface temperature of the cylinder was rapidly cooled from 300°C to room temperature. The local metal temperature at the location of the deepest intergranular cracking was dropping towards 100°C when the crack driving force was approaching its peak. The fact that intergranular fracture was absent in any of the present tests at 120°C (both those with continuous hydrogenation during testing or those with pre-hydrogenation) suggests that hydrogen embrittlement is unlikely to have caused the observed cracking in the NESC cylinder under these conditions.

Conclusions

The fracture and stress corrosion cracking tests demonstrated a detrimental effect of both hydrogenation during testing and pre-hydrogenation on the J_{Ii} or K_{Ith} levels for the HAZ and sub-HAZ base materials. This implies that susceptibility to sub-critical cracking may need to be considered for real or postulated defects in embrittled components subject to such conditions over extended periods. The SSC results suggest that the base material is more sensitive to hydrogen embrittlement effects than the HAZ; this is considered to be linked to the presence of segregation bands in the former. Fractographic examination shows that the effect of hydrogen becomes apparent as classical embrittlement (cleavage, intercrystalline or intergranular fracture) only in the transition regime (ambient temperature for this steel). At the 120°C test temperature (upper shelf) hydrogen charging appears to reduce the energy needed for ductile tearing along slip planes, with much finer dimpling than found in the absence of environment effects. There is some evidence that pre-absorbed hydrogen favours local cleavage. Differences in fracture mode for hydrogenated specimens at the two temperature levels is also thought to be connected with a competition between two types of hydrogen transport to the crack tip – by grain boundary diffusion and via mobile dislocations in the bulk. The former is prevalent at ambient temperature when intergranular fracture is observed.

References

[1] R. Hurst, N. Taylor, D. McGarry, B. R. Brass, R. Rintamaa, J. Wintle: Int. J. Pressure Vessels and Piping, **78** (2001), p. 213.

[2] O.T. Tsyrulnyk, E.I. Kryzhanivskyi, D.Yu. Petryna, O.S. Taraevskyi, M.I. Hredil: Material Science, No. 6 (2004), p. 844.

[3] Schuring E.W: Report No. ECN-I-97-047, March 1998.